The Quadratic-Chi Histogram Distance Family - Appendices

Ofir Pele and Michael Werman

School of Computer Science
The Hebrew University of Jerusalem
{ofirpele,werman}@cs.huji.ac.il

1 Introduction

This document contains the appendices for the paper "The Quadratic-Chi Histogram Distance Family" [1], proofs and additional results. In section 2 we prove that all Quadratic-Chi histogram distances are continuous. In section 3 we prove that EMD, $\widehat{\text{EMD}}$ and all Quadratic-Chi histogram distances are *Similarity-Matrix-Quantization-Invariant*. In section 4 we present additional shape classification results. In section 5 we compare experimentally color image distances with and without spatial pruning. In section 6 we compare experimentally distances which resembles QC distances, but are either not *Similarity-Matrix-Quantization-Invariant* or not *Sparseness-Invariant*. In section 7 we compare the results for all the pairs of descriptors (SIFT/CSIFT) and distance measures used in the image retrieval experiments.

2 Quadratic-Chi Histogram Distance Continuity Proof

In this section we prove that a Quadratic-Chi (QC) histogram distance is continuous. We first recall its definition.

Let P and Q be two non-negative bounded histograms. That is, $P, Q \in [0, U]^N$, where the bound U can be any finite number. Let A be a non-negative symmetric bounded bin-similarity matrix such that each diagonal element is bigger or equal to every other element in its row (this demand is weaker than being a strongly dominant matrix) and to 1. That is, $A \in [0, U]^N \times [0, U]^N$ and $\forall i, j \; A_{ii} \geq A_{ij}$ and $\forall i \; A_{ii} \geq 1$. Let $0 \leq m < 1$ be the normalization factor. A Quadratic-Chi (QC) histogram distance is defined as:

$$\text{QC}_m^A(P, Q) = \sqrt{\sum_{ij} \left(\frac{(P_i - Q_i)}{\left(\sum_c (P_c + Q_c) A_{ci}\right)^m} \right) \left(\frac{(P_j - Q_j)}{\left(\sum_c (P_c + Q_c) A_{cj}\right)^m} \right) A_{ij}} \quad (1)$$

Theorem 1. *Each addend denominator:* $(\sum_c (P_c + Q_c) A_{ci})^m (\sum_c (P_c + Q_c) A_{cj})^m$*, is zero only if the addend numerator:* $(P_i - Q_i)(P_j - Q_j) A_{ij}$*, is zero.*

Proof.

$$(\sum_c (P_c+Q_c)A_{ci})^m (\sum_c (P_c+Q_c)A_{cj})^m = 0 \quad \Rightarrow \tag{2}$$
$$((P_i+Q_i)A_{ii})^m ((P_j+Q_j)A_{jj})^m = 0 \quad \Rightarrow \tag{3}$$
$$(P_i = 0 \wedge Q_i = 0) \vee (P_j = 0 \wedge Q_j = 0) \quad \Rightarrow \tag{4}$$
$$((P_i - Q_i) = 0) \vee ((P_j - Q_j) = 0) \quad \Rightarrow \tag{5}$$
$$(P_i - Q_i)(P_j - Q_j)A_{ij} = 0 \tag{6}$$

Eqs. 3,4 and 6 are true as everything is non-negative and $A_{ii} \geq 1$.

We defined $\frac{0}{0} = 0$. So, in order to prove continuity, we need to prove that when QC addend's denominator tends to zero, the whole addend tends to zero (this is the only point where discontinuity can occur).

Theorem 2.

$$\begin{gathered}(\sum_c (P_c+Q_c)A_{ci})^m (\sum_c (P_c+Q_c)A_{cj})^m \to 0 \Rightarrow \\ \left(\frac{(P_i - Q_i)}{(\sum_c (P_c+Q_c)A_{ci})^m}\right)\left(\frac{(P_j - Q_j)}{(\sum_c (P_c+Q_c)A_{cj})^m}\right) A_{ij} \to 0\end{gathered} \tag{7}$$

Proof.

$$(\sum_c (P_c+Q_c)A_{ci})^m (\sum_c (P_c+Q_c)A_{cj})^m \to 0 \quad \Rightarrow \tag{8}$$
$$((P_i+Q_i)A_{ii})^m ((P_j+Q_j)A_{jj})^m \to 0 \quad \Rightarrow \tag{9}$$
$$((P_i+Q_i)^m \to 0) \vee ((P_j+Q_j)^m \to 0) \quad \Rightarrow \tag{10}$$
$$\big((P_i \to 0) \wedge (Q_i \to 0)\big) \vee \big((P_j \to 0) \wedge (Q_j \to 0)\big) \quad \Rightarrow \tag{11}$$
$$\left(\frac{(P_i - Q_i)}{((P_i+Q_i)A_{ii})^m}\right)\left(\frac{(P_j - Q_j)}{((P_j+Q_j)A_{jj})^m}\right) A_{ij} \to 0 \quad \Rightarrow \tag{12}$$
$$\left(\frac{(P_i - Q_i)}{(\sum_c (P_c+Q_c)A_{ci})^m}\right)\left(\frac{(P_j - Q_j)}{(\sum_c (P_c+Q_c)A_{cj})^m}\right) A_{ij} \to 0 \quad \Rightarrow \tag{13}$$

Eq. 9 is true as everything is non-negative and $m \geq 0$. Eq. 10 is true as if the whole product tends to zero, at least one of its multiplicands should tend to zero and $A_{ii} \geq 1$ and $A_{jj} \geq 1$. Eq. 11 is true as everything is non-negative and $m \geq 0$. Eq. 12 is true as $|(P_i - Q_i)| \leq |(P_i + Q_i)|A_{ii}$ and $|(P_j - Q_j)| \leq |(P_j + Q_j)|A_{jj}$ and $0 \leq m < 1$ (note that the strictly smaller than one is required here) and everything is bounded. Eq. 13 finishes the proof and is true as:

$$\left|\left(\frac{(P_i - Q_i)}{(\sum_c (P_c+Q_c)A_{ci})^m}\right)\right| < \left|\left(\frac{(P_i - Q_i)}{((P_i+Q_i)A_{ii})^m}\right)\right| \wedge \tag{14}$$
$$\left|\left(\frac{(P_j - Q_j)}{(\sum_c (P_c+Q_c)A_{cj})^m}\right)\right| < \left|\left(\frac{(P_j - Q_j)}{((P_j+Q_j)A_{jj})^m}\right)\right| \tag{15}$$

3 EMD, $\widehat{\text{EMD}}$ and Quadratic-Chi Histogram Distances *Similarity-Matrix-Quantization-Invariance* Proof

In this section we prove that EMD, $\widehat{\text{EMD}}$ and all Quadratic-Chi histogram distances are *Similarity-Matrix-Quantization-Invariant*. We recall *Similarity-Matrix-Quantization-Invariance* definition:

Definition 1. *Let $\mathcal{D}$ be a cross-bin histogram distance between two histograms P and Q and let A be the bin-similarity/distance matrix. We assume P, Q and A are non-negative and that A is symmetric. Let $A_{k,:}$ be the kth row of A. Let $V = [V_1, \dots, V_N]$ be a non-negative vector and $0 \le \alpha \le 1$. We define $V^{\alpha,k,b} = [\dots, \alpha V_k, \dots, V_b + (1-\alpha)V_k, \dots]$. That is, $V^{\alpha,k,b}$ is a transformation of V where $(1-\alpha)V_k$ mass has moved from bin k to bin b. We define $\mathcal{D}$ to be* Similarity-Matrix-Quantization-Invariant *if:*

$$A_{k,:} = A_{b,:} \Rightarrow \forall \; 0 \le \alpha \le 1, \; 0 \le \beta \le 1 \quad \mathcal{D}^A(P,Q) = \mathcal{D}^A(P^{\alpha,k,b}, Q^{\beta,k,b}) \tag{16}$$

If $\mathcal{D}$ is symmetric then Eq. 16 is equivalent to:

$$A_{k,:} = A_{b,:} \Rightarrow \forall \; 0 \le \alpha \le 1 \quad \mathcal{D}^A(P,Q) = \mathcal{D}^A(P^{\alpha,k,b}, Q) \tag{17}$$

EMD [2] and $\widehat{\text{EMD}}$ [3] distances are *Similarity-Matrix-Quantization-Invariant*. Since both are min-cost-flow problems [4], taking mass from one source/sink and moving it to another one, where both sources/sinks are connected to exactly the same sinks/sources, with exactly the same costs, will not change the min-cost solution.

We begin the proof that a Quadratic-Chi (QC) histogram distance (Eq. 1) is *Similarity-Matrix-Quantization-Invariant* with a lemma:

$$(\sum_c (P_c^{\alpha,k,b} + Q_c) A_{ci})^m = (\sum_c (P_c + Q_c) A_{ci})^m \tag{18}$$

Proof.

$$\sum_c (P_c^{\alpha,k,b} + Q_c) A_{ci} = \tag{19}$$

$$\Big(\sum_{c \ne k,b} (P_c^{\alpha,k,b} + Q_c) A_{ci}\Big) + \Big((P_k^{\alpha,k,b} + Q_k) A_{ki}\Big) + \Big((P_b^{\alpha,k,b} + Q_b) A_{bi}\Big) = \tag{20}$$

$$\Big(\sum_{c \ne k,b} (P_c + Q_c) A_{ci}\Big) + \Big((\alpha P_k + Q_k) A_{ki}\Big) + \Big((P_b + (1-\alpha) P_k + Q_b) A_{bi}\Big) = \tag{21}$$

$$\Big(\sum_{c \ne k,b} (P_c + Q_c) A_{ci}\Big) + \Big((\alpha P_k + Q_k) A_{ki}\Big) + \Big((P_b + (1-\alpha) P_k + Q_b) A_{ki}\Big) = \tag{22}$$

$$\Big(\sum_{c \ne k,b} (P_c + Q_c) A_{ci}\Big) + \Big((P_k + Q_k + P_b + Q_b) A_{ki}\Big) = \tag{23}$$

$$\Big(\sum_{c \ne k,b} (P_c + Q_c) A_{ci}\Big) + \Big((P_k + Q_k) A_{ki}\Big) + \Big((P_b + Q_b) A_{bi}\Big) = \tag{24}$$

$$\sum_c (P_c + Q_c) A_{ci} \tag{25}$$

$$\Updownarrow \tag{26}$$

$$(\sum_c (P_c^{\alpha,k,b} + Q_c) A_{ci})^m = (\sum_c (P_c + Q_c) A_{ci})^m \tag{27}$$

In the proof we use the definitions and in Eqs. 22,24 we use $A_{ki} = A_{bi}$.

We now prove that Quadratic-Chi histogram distance is *Similarity-Matrix-Quantization-Invariant* using Eq. 17. That is we prove that:

$$A_{k,:} = A_{b,:} \;\Rightarrow\; \forall \;\; 0 \leq \alpha \leq 1 \quad QC_m^A(P,Q) = QC_m^A(P^{\alpha,k,b},Q) \tag{28}$$

We will prove that $(QC_m^A(P,Q))^2 = (QC_m^A(P^{\alpha,k,b},Q))^2$ which directly implies Eq. 28.

We start by separating $(QC_m^A(P^{\alpha,k,b},Q))^2$ addends into three disjoint and complementary types. The first type is when both i and j are different from k and b. For these addends the equality is direct from the definition. The second type is when both i and j are either k or b. For this type the proof is:

$$\sum_{i=(k\vee b),j=(k\vee b)} \frac{(P_i^{\alpha,k,b}-Q_i)(P_j^{\alpha,k,b}-Q_j)A_{ij}}{\left(\sum_c (P_c^{\alpha,k,b}+Q_c)A_{ci}\right)^m \left(\sum_c (P_c^{\alpha,k,b}+Q_c)A_{cj}\right)^m} = \tag{29}$$

$$\sum_{i=(k\vee b),j=(k\vee b)} \frac{(P_i^{\alpha,k,b}-Q_i)(P_j^{\alpha,k,b}-Q_j)A_{ij}}{\left(\sum_c (P_c+Q_c)A_{ci}\right)^m \left(\sum_c (P_c+Q_c)A_{cj}\right)^m} = \tag{30}$$

$$\frac{(P_k^{\alpha,k,b}-Q_k)(P_k^{\alpha,k,b}-Q_k)A_{kk}}{\left(\sum_c (P_c+Q_c)A_{ck}\right)^{2m}} + \frac{(P_k^{\alpha,k,b}-Q_k)(P_b^{\alpha,k,b}-Q_b)A_{kb}}{\left(\sum_c (P_c+Q_c)A_{ck}\right)^m \left(\sum_c (P_c+Q_c)A_{cb}\right)^m} +$$

$$\frac{(P_b^{\alpha,k,b}-Q_b)(P_k^{\alpha,k,b}-Q_k)A_{bk}}{\left(\sum_c (P_c+Q_c)A_{cb}\right)^m \left(\sum_c (P_c+Q_c)A_{ck}\right)^m} + \frac{(P_b^{\alpha,k,b}-Q_b)(P_b^{\alpha,b,b}-Q_b)A_{bb}}{\left(\sum_c (P_c+Q_c)A_{cb}\right)^{2m}} = \tag{31}$$

$$\frac{\Big((\alpha P_k - Q_k)^2 + 2(\alpha P_k - Q_k)((P_b+(1-\alpha)P_k)-Q_b) + ((P_b+(1-\alpha)P_k)-Q_b)^2\Big)A_{kk}}{\left(\sum_c (P_c+Q_c)A_{ck}\right)^{2m}} = \tag{32}$$

$$\frac{\Big((\alpha P_k - Q_k) + ((P_b+(1-\alpha)P_k)-Q_b)\Big)^2 A_{kk}}{\left(\sum_c (P_c+Q_c)A_{ck}\right)^{2m}} = \tag{33}$$

$$\frac{\Big((P_k - Q_k) + (P_b-Q_b)\Big)^2 A_{kk}}{\left(\sum_c (P_c+Q_c)A_{ck}\right)^{2m}} = \tag{34}$$

$$\frac{\Big((P_k - Q_k)^2 + 2(P_k-Q_k)(P_b-Q_b) + (P_b-Q_b)^2\Big)A_{kk}}{\left(\sum_c (P_c+Q_c)A_{ck}\right)^{2m}} = \tag{35}$$

$$\sum_{i=(k\vee b),j=(k\vee b)} \frac{(P_i-Q_i)(P_j-Q_j)A_{ij}}{\left(\sum_c (P_c+Q_c)A_{ci}\right)^m \left(\sum_c (P_c+Q_c)A_{cj}\right)^m} \tag{36}$$

Eq. 30 is based on the lemma in Eq. 18. Eqs. 32,36 are true as $A_{ck} = A_{cb}$ and $A_{kk} = A_{kb} = A_{bb} = A_{bk}$.

The third type of addends is when only i equals b or k or only j equals b or k. These sub-cases are symmetric, so it is enough to prove equality for only one of them:

$$\sum_{i=(k\vee b),j\neq(k\vee b)} \frac{(P_i^{\alpha,k,b}-Q_i)(P_j^{\alpha,k,b}-Q_j)A_{ij}}{\left(\sum_c(P_c^{\alpha,k,b}+Q_c)A_{ci}\right)^m\left(\sum_c(P_c^{\alpha,k,b}+Q_c)A_{cj}\right)^m} = \tag{37}$$

$$\sum_{i=(k\vee b),j\neq(k\vee b)} \frac{(P_i^{\alpha,k,b}-Q_i)(P_j-Q_j)A_{ij}}{\left(\sum_c(P_c+Q_c)A_{ci}\right)^m\left(\sum_c(P_c+Q_c)A_{cj}\right)^m} = \tag{38}$$

$$\sum_{j\neq(k\vee b)} \left(\frac{(P_k^{\alpha,k,b}-Q_k)(P_j-Q_j)A_{kj}}{\left(\sum_c(P_c+Q_c)A_{ck}\right)^m\left(\sum_c(P_c+Q_c)A_{cj}\right)^m} + \frac{(P_b^{\alpha,k,b}-Q_b)(P_j-Q_j)A_{bj}}{\left(\sum_c(P_c+Q_c)A_{cb}\right)^m\left(\sum_c(P_c+Q_c)A_{cj}\right)^m} \right) = \tag{39}$$

$$\sum_{j\neq(k\vee b)} \left(\frac{(\alpha P_k-Q_k+(P_b+(1-\alpha)P_k)-Q_b)(P_j-Q_j)A_{kj}}{\left(\sum_c(P_c+Q_c)A_{ck}\right)^m\left(\sum_c(P_c+Q_c)A_{cj}\right)^m} \right) = \tag{40}$$

$$\sum_{j\neq(k\vee b)} \left(\frac{((P_k-Q_k)+(P_b-Q_b))(P_j-Q_j)A_{kj}}{\left(\sum_c(P_c+Q_c)A_{ck}\right)^m\left(\sum_c(P_c+Q_c)A_{cj}\right)^m} \right) = \tag{41}$$

$$\sum_{i=(k\vee b),j\neq(k\vee b)} \frac{(P_i-Q_i)(P_j-Q_j)A_{ij}}{\left(\sum_c(P_c+Q_c)A_{ci}\right)^m\left(\sum_c(P_c+Q_c)A_{cj}\right)^m} \tag{42}$$

Eq. 38 is based on the lemma in Eq. 18. Eqs. 40,42 are true as $A_{kj} = A_{bj}$ and $A_{ck} = A_{cb}$.

Since we covered the three disjoint and complementary cases we have proved that a Quadratic-Chi histogram distance is *Similarity-Matrix-Quantization-Invariant*.

4 Additional Shape Classification Results

This section presents shape classification results using the same framework as Ling et al. [5,6,7]. We first present results for the articulated shape data set [5,7]. Then we present results for the Kimia-216 data set [8].

4.1 Articulated Data Set

The articulated shape data set [5,7] has 40 images from 8 different objects. Each object has 5 images articulated to different degrees, see Fig. 1(a). The dataset is very challenging because of the similarity between different objects (especially the scissors).

We used Belongie et al.'s Shape Context (SC) [9] and Ling and Jacobs' Inner Distance Shape Context (IDSC) [5].

To evaluate results, for each image, the 4 most similar matches are chosen from other images in the dataset. The retrieval result is summarized as the number of 1st,

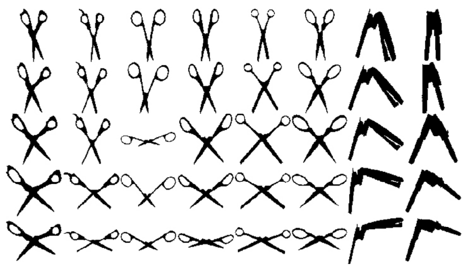

(a)

Results using SC[9]

	Top 1	Top 2	Top 3	Top 4	AUC%
QCN$^{1-\frac{\mathrm{dsc}_{T=2}}{2}}$	20	6	10	5	0.307
QCN^{I}	18	7	5	8	0.278
QCS$^{1-\frac{\mathrm{dsc}_{T=2}}{2}}$	23	11	11	4	0.378
QCS^{I}	19	9	9	6	0.318
χ^2	25	13	13	7	0.430
$QF^{1-\frac{\mathrm{dsc}_{T=2}}{2}}$	25	16	10	7	0.438
L_2	25	15	8	7	0.420
$\widehat{\mathrm{EMD}}_1^{\mathrm{dsc}_{T=2}}$	23	13	11	7	0.400
L_1	20	10	9	5	0.333
SIFT$_{\mathrm{DIST}}$[10]	20	9	6	9	0.320
EMD-L_1[6]	15	10	6	10	0.280
Diffusion[11]	19	10	7	6	0.315
Bhattacharyya[12]	25	14	9	9	0.422
KL[13]	12	8	4	9	0.223
JS[14]	25	16	9	7	0.432

(b)

Results using IDSC[5]

	Top 1	Top 2	Top 3	Top 4	AUC%
QCN$^{1-\frac{\mathrm{dsc}_{T=2}}{2}}$	39	38	38	34	0.950
QCN^{I}	40	37	36	33	0.940
QCS$^{1-\frac{\mathrm{dsc}_{T=2}}{2}}$	39	35	38	28	0.912
QCS^{I}	40	34	37	27	0.907
χ^2	40	36	36	21	0.902
$QF^{1-\frac{\mathrm{dsc}_{T=2}}{2}}$	40	34	39	19	0.897
L_2	39	35	35	18	0.873
$\widehat{\mathrm{EMD}}_1^{\mathrm{dsc}_{T=2}}$	39	36	35	27	0.902
L_1	39	35	35	25	0.890
SIFT$_{\mathrm{DIST}}$[10]	38	37	27	22	0.848
EMD-L_1[6]	39	35	38	30	0.917
Diffusion[11]	39	35	34	23	0.880
Bhattacharyya[12]	40	37	32	23	0.895
KL[13]	40	38	36	29	0.938
JS[14]	40	35	37	21	0.900

(c)

Fig. 1. (a) Articulated shape database. This dataset contains 40 images from 8 objects. Each column contains five images of the same object with different articulation.
(b) Shape classification results using Belongie et al.'s Shape Context (SC)[9]. All distances performance is poor.
(c) Shape classification results using Ling and Jacobs' Inner Distance Shape Context (IDSC)[5]. QCN$^{1-\frac{\mathrm{dsc}_{T=2}}{2}}$ outperformed all other distances. QCN^{I} performance was excellent, which shows the importance of the normalization factor. All cross-bin distances outperformed their bin-by-bin versions. Again, χ^2 and QF improved upon L_2. QCN and QCS which are mathematically sound combinations of χ^2 and QF outperformed both.

2nd, 3rd and 4th most similar matches that come from the correct object. Tables (b) and (c) in Fig. 1 show the retrieval results for SC and IDSC respectively. Using SC descriptors, the performance was poor on this dataset for all kinds of distances. Using IDSC descriptors, the $\mathrm{QCN}^{1-\frac{\mathrm{dsc}_{T=2}}{2}}$ histogram distance outperformed all the other distances. QCN^{I} performance was excellent, which shows the importance of the normalization factor. All cross-bin distances outperformed their bin-by-bin versions. χ^2 and QF improved upon L_2. QCN and QCS which are mathematically sound combinations of χ^2 and QF outperformed both.

4.2 Kimia-216 Data Set

The Kimia-216 shape data set [8] has 216 images grouped into 18 classes with 12 images in each class, see Fig. 2(a).

We tested for shape classification with Belongie et al. Shape Context (SC) [9]. We do not present results for Ling and Jacob's IDSC [5], as the code that computes IDSC [7] crashes on this data set (segmentation fault).

To evaluate results, for each image, the 11 most similar matches are chosen from other images in the dataset (as there are 12 images in each class). The retrieval result is summarized as the number of 1st, 2nd, ..., 11th and most similar matches that come from the correct object. Table (b) in Fig. 2(b) show the retrieval results. Again, the $\mathrm{QCN}^{1-\frac{\mathrm{dsc}_{T=2}}{2}}$ histogram distance outperformed all the other distances. Again, χ^2 and QF improved upon L_2 and QCN and QCS outperformed both.

5 Comparison of Color Image Distances With and Without Spatial Pruning

In this section we compare experimentally the color image distances that have spatial pruning (those used in [1]) to distances without such a pruning (those used in [3]). Results are presented in Fig. 3. Pruning slightly improved accuracy for QF and slightly reduced accuracy for QCN, QCS and $\widehat{\mathrm{EMD}}$. However, pruning considerably reduced running time (see Table 1 in page 15).

6 Comparison to *Non-Similarity-Matrix-Quantization-Invariant* and *Non-Sparseness-Invariant* Quadratic-Chi-like Histogram Distances

In this section we compare experimentally distances which resembles QC distances, but are either not *Similarity-Matrix-Quantization-Invariant* or not *Sparseness-Invariant*. The comparison shows that these properties considerably boost performance, especially for sparse color histograms.

As in the QC definition, let P and Q be two non-negative bounded histograms. That is, $P, Q \in [0, U]^N$. Let A be a non-negative symmetric bounded bin-similarity matrix such that each diagonal element is bigger or equal to every other element in its

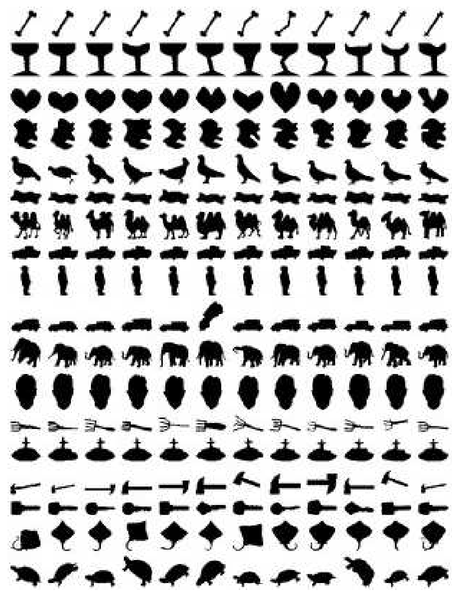

(a)

Results using SC[9]

	Top 1	Top 2	Top 3	Top 4	Top 5	Top 6	Top 7	Top 8	Top 9	Top 10	Top 11	AUC%
$\mathrm{QCN}^{1-\frac{\mathrm{dsc}_{T=2}}{2}}$	215	216	215	216	214	214	207	207	200	192	173	0.981
QCN^{I}	215	208	212	201	198	198	190	177	164	150	127	0.920
$\mathrm{QCS}^{1-\frac{\mathrm{dsc}_{T=2}}{2}}$	216	215	215	212	212	205	204	205	193	184	155	0.969
QCS^{I}	215	215	214	214	215	208	209	205	197	190	167	0.976
χ^2	216	215	212	211	210	203	199	199	192	177	156	0.960
$QF^{1-\frac{\mathrm{dsc}_{T=2}}{2}}$	214	211	207	206	197	190	183	183	167	162	146	0.920
L_2	213	210	203	204	195	189	183	178	167	149	139	0.910
$\widehat{\mathrm{EMD}}_1^{\mathrm{dsc}_{T=2}}$	215	215	215	215	214	207	207	202	201	187	162	0.974
L_1	215	215	215	214	213	209	211	207	199	192	170	0.978
$\mathrm{SIFT}_{\mathrm{DIST}}$[10]	215	215	215	215	215	211	210	207	201	189	162	0.979
EMD-L_1[6]	215	215	212	213	212	208	204	203	197	184	161	0.969
Diffusion[11]	215	215	214	214	214	214	208	204	200	196	174	0.979
Bhattacharyya[12]	216	215	213	212	212	206	203	206	193	177	159	0.967
KL[13]	212	203	200	199	195	186	187	179	166	151	130	0.899
JS[14]	216	215	212	210	208	205	200	197	189	182	152	0.959

(b)

Fig. 2. (a) Kimia-216 shape database. This dataset has 216 images from 18 classes. Each row contains 12 images of the same class.
(b) Shape classification results using the Shape Context (SC)[9]. We do not present results for Ling and Jacob's IDSC [5], as the code that computes IDSC [7] crashed (segmentation fault). Again, the $\mathrm{QCN}^{1-\frac{\mathrm{dsc}_{T=2}}{2}}$ histogram distance outperformed all other distances. Again, χ^2 and QF improved upon L_2. QCN and QCS which are mathematically sound combinations of χ^2 and QF outperformed both.

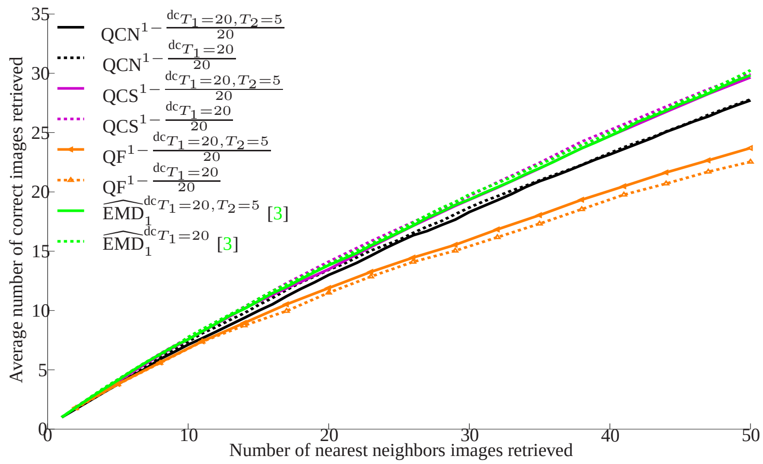

Fig. 3. Results for image retrieval comparing distances which are pruning spatially far away pixels (painted with solid lines) to those that are not (painted with broken lines). Pruning slightly improved accuracy for QF and slightly reduced accuracy for QCN, QCS and $\widehat{\mathrm{EMD}}$. However, pruning considerably reduced running time (see Table 1 in page 15).

row (this demand is weaker than being a strongly dominant matrix) and to 1. That is, $A \in [0, U]^N \times [0, U]^N$ and $\forall i, j \;\; A_{ii} \geq A_{ij}$ and $\forall i \;\; A_{ii} \geq 1$. Let $0 \leq m < 1$ be the normalization factor. A QC-like histogram distance which is not *Sparseness-Invariant* is defined as:

$$\text{NSI-QC}_m^A(P,Q) = \sqrt{\sum_{ij} \left(\frac{\left(\sum_c P_c A_{ci} - \sum_c Q_c A_{ci}\right)}{\left(\sum_c (P_c + Q_c) A_{ci}\right)^m} \right) \left(\frac{\left(\sum_c P_c A_{cj} - \sum_c Q_c A_{cj}\right)}{\left(\sum_c (P_c + Q_c) A_{cj}\right)^m} \right) A_{ij}} \tag{43}$$

A QC-like histogram distance which is not *Similarity-Matrix-Quantization-Invariant* is defined as:

$$\text{NQI-QC}_m^A(P,Q) = \sqrt{\sum_{ij} \left(\frac{(P_i - Q_i)}{(P_i + Q_i)^m} \right) \left(\frac{(P_j - Q_j)}{(P_j + Q_j)^m} \right) A_{ij}} \tag{44}$$

If I is the identity matrix then:

$$\text{QC}_m^I(P,Q) = \text{NSI-QC}_m^I(P,Q) = \text{NQI-QC}_m^I(P,Q) \tag{45}$$

For any bin-similarity A we get the following equality:

$$\text{NQI-QC}_m^I(AP, AQ) = \text{NSI-QC}_m^I(P,Q) \tag{46}$$

We present results for image retrieval comparing QCN, NSI-QCN(NSI-QC$_{0.9}$), NQI-QCN(NQI-QC$_{0.9}$), QCS, NSI-QCS(NSI-QC$_{0.5}$) and NQI-QCS(NQI-QC$_{0.5}$) in Fig. 4(a) for SIFT-like descriptors (CSIFT as the CSIFT descriptor, compared to SIFT was better for all distance measures, see Fig. 7) and in Fig. 4(b) for small L*a*b* images with the pruning distance used in the paper [1] and in 4(c) for small L*a*b* images with a non-pruning distance as was used in [3]. The results show that *Similarity-Matrix-Quantization-Invariance* and *Sparseness-Invariance* considerably boost performance. The gain in performance is large using the L*a*b* images, which are sparse 5-dimensional histograms (x, y, L*, a*, b*). That is, the query histogram was always: $[1, \ldots, 1, 0, \ldots, 0]$ and each image being compared to the query was represented by the histogram: $[0, \ldots, 0, 1, \ldots, 1]$. That is, the dimension of the space is $32 \times 48 \times 256^3$ where only 32×48 entries are non-zero in each histograms. The bin-similarity matrix is computed for each pair of images. For these histograms:

$$\text{NQI-QCN}^A(P,Q) = \text{NQI-QCS}^A(P,Q) = \text{QF}^A(P,Q) \tag{47}$$

The time complexity of all the distances tested in this section is linear. In practice (see Table 1), QCS distances are faster to compute than QCN distances. In addition, NQI-QC distances are the fastest to compute, QC distances second, and NSI-QC distances have the longest running time. However, the differences between the running times are minor as all distances have linear time complexity.

7 Comparing SIFT/CSIFT with All Distances for Image Retrieval

In this section we present results for image retrieval as described in the paper. The results are for all pairs of descriptors (SIFT/CSIFT) and distance measures and given in Figs. 5, 6,7.

References

1. Pele, O., Werman, M.: The quadratic-chi histogram distance family. In: ECCV. (2010) 1, 7, 10
2. Rubner, Y., Tomasi, C., Guibas, L.J.: The earth mover's distance as a metric for image retrieval. IJCV (2000) 3
3. Pele, O., Werman, M.: Fast and robust earth mover's distances. In: ICCV. (2009) 3, 7, 9, 10, 13
4. Ahuja, R., Magnanti, T., Orlin, J.: Network flows: theory, algorithms, and applications. (1993) 3
5. Ling, H., Jacobs, D.: Shape classification using the inner-distance. PAMI (2007) 5, 6, 7, 8
6. Ling, H., Okada, K.: An Efficient Earth Mover's Distance Algorithm for Robust Histogram Comparison. PAMI (2007) 5, 6, 8, 13
7. Ling, H.: Articulated shape benchmark and idsc code. http://www.ist.temple.edu/~hbling/code/inner-dist-articu-distrbution.zip (2010) 5, 7, 8
8. Sebastian, T., Kimia, B.: Curves vs. skeletons in object recognition. SP (2005) 5, 7
9. Belongie, S., Malik, J., Puzicha, J.: Shape matching and object recognition using shape contexts. PAMI (2002) 5, 6, 7, 8

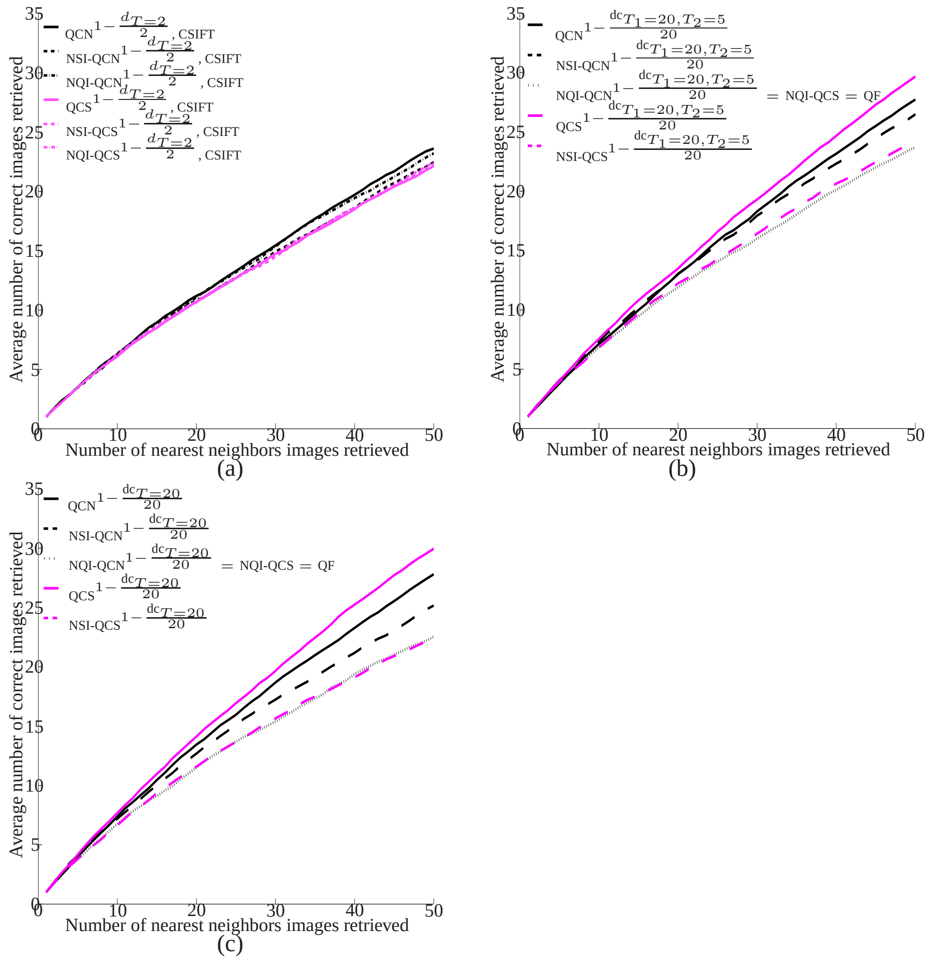

Fig. 4. Results for image retrieval comparing QC which is *Sparseness-Invariant* and *Similarity-Matrix-Quantization-Invariant* to NSI-QC and to NQI-QC which are not *Sparseness-Invariant* and not *Similarity-Matrix-Quantization-Invariant* respectively.
(a) **SIFT-like descriptors.** For each distance measure, we present the descriptor (SIFT/CSIFT) with which it performed best. The results for all the pairs of descriptors and distance measures can be found in Figs. 5, 6 and 7. It can be seen that QCN which is both *Sparseness-Invariant* and *Similarity-Matrix-Quantization-Invariant* has the best performance. However, the differences in performance are small.
(b) **L*a*b* images with pruning and (c) without pruning** Here, the *Sparseness-Invariant* and *Similarity-Matrix-Quantization-Invariant* properties are very important. This is probably because L*a*b* images are represented as very sparse histograms in a very high dimensional space (the dimension of the space is $32 \times 48 \times 256^3$ where only 32×48 entries are non-zero in each histograms). Comparing to (b) we can also note that performance using this representation is better than those obtained with the SIFT-like descriptor.

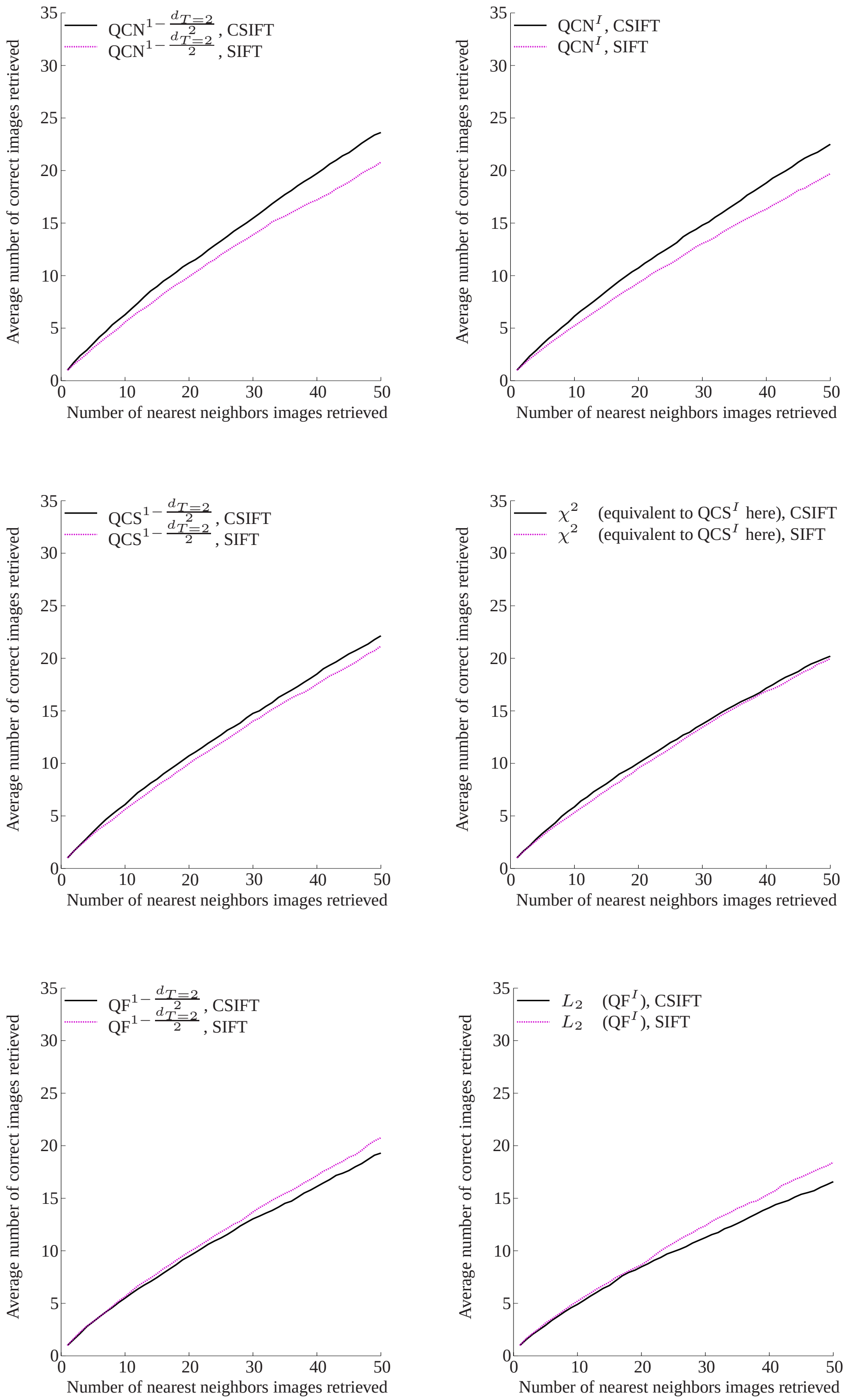

Fig. 5. Comparison of SIFT with CSIFT for all distances, part 1.

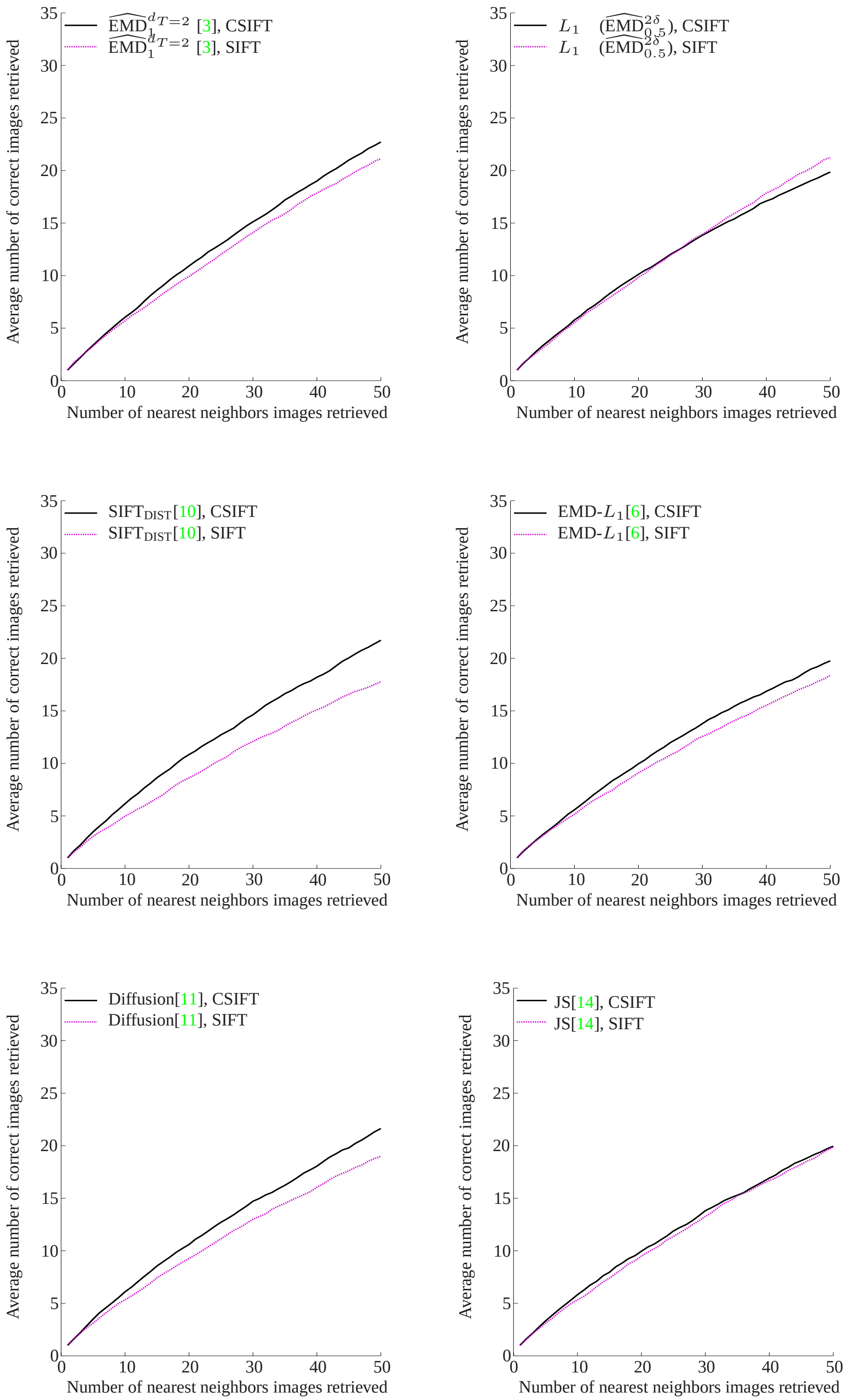

Fig. 6. Comparison of SIFT with CSIFT for all distances, part 2

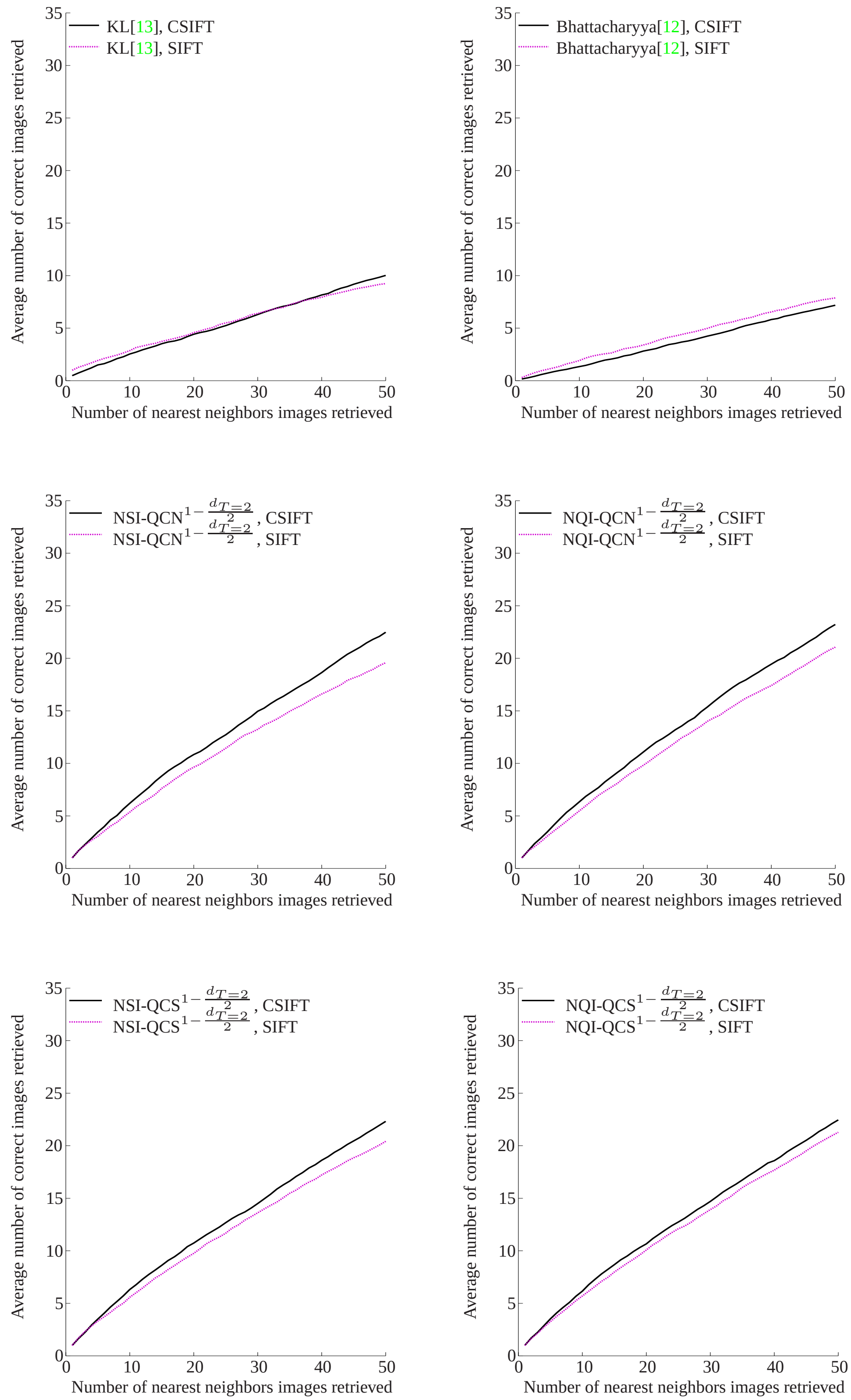

Fig. 7. Comparison of SIFT with CSIFT for all distances, part 3

Descriptor	QCN^{A_2}	NSI-QCN^{A_2}	NQI-QCN^{A_2}	QCS^{A_2}	NSI-QCS^{A_2}	NQI-QCS^{A_2}
(SIFT)	**0.15**	**0.18**	**0.14**	**0.07**	**0.1**	**0.06**

Descriptor	$QCN^{A_{20,5}}$	NSI-$QCN^{A_{20,5}}$	$QF^{A_{20,5}}$	$QCS^{A_{20,5}}$	NSI-$QCS^{A_{20,5}}$
(L*a*b*)	**20** (370)	**21** (371)	**11** (361)	**19** (369)	**18** (368)

Descriptor	$QCN^{A_{20}}$	NSI-$QCN^{A_{20}}$	$QF^{A_{20}}$	$QCS^{A_{20}}$	NSI-$QCS^{A_{20}}$
(L*a*b*)	**20** (3020)	**21** (3021)	**11** (3011)	**19** (3019)	**18** (3018)

Table 1. (SIFT) 384-dimensional SIFT-like descriptors matching time (in *milliseconds*). The distances from left to right are the same as the distances in Fig. 4 (a) from up to down.
(L*a*b*) 32×48 L*a*b* images matching time (in *milliseconds*) using a distance which prunes spatially far away pixels (middle row) and a distance which does not (bottom row). On the middle row, the distances from left to right are the same as the distances in Fig. 4 (b). On the bottom row, the distances from left to right are the same as the distances in Fig. 4 (c). In parentheses is the time it takes to compute the distance and the bin-similarity matrix as it cannot be computed offline.

To summaries results, QCS distances are faster to compute than QCN distances. Also, NQI-QC distances are the fastest to compute, QC distances second, and NSI-QC distances have the longest running time. However, the differences between the running times are minor as all distances have linear time complexity. Finally, pruning spatially far away pixels considerably reduced running time, almost without reducing accuracy (see Fig. 3).

10. Pele, O., Werman, M.: A linear time histogram metric for improved sift matching. In: ECCV. (2008) 6, 8, 13
11. Ling, H., Okada, K.: Diffusion distance for histogram comparison. In: CVPR. (2006) 6, 8, 13
12. Bhattacharyya, A.: On a measure of divergence between two statistical populations defined by their probability distributions. BCMS (1943) 6, 8, 14
13. Kullback, S., Leibler, R.: On information and sufficiency. AMS (1951) 6, 8, 14
14. Lin, J.: Divergence measures based on the Shannon entropy. IT (1991) 6, 8, 13